

**General implementation of arbitrary nonlinear quadrature phase gates**Petr Marek,<sup>1,\*</sup> Radim Filip,<sup>1</sup> Hisashi Ogawa,<sup>2</sup> Atsushi Sakaguchi,<sup>2</sup> Shuntaro Takeda,<sup>2</sup> Jun-ichi Yoshikawa,<sup>2,3</sup> and Akira Furusawa<sup>2,†</sup><sup>1</sup>*Department of Optics, Palacký University, 17. listopadu 1192/12, 77146 Olomouc, Czech Republic*<sup>2</sup>*Department of Applied Physics, School of Engineering, The University of Tokyo, 7-3-1 Hongo, Bunkyo-ku, Tokyo 113-8656, Japan*<sup>3</sup>*Quantum-Phase Electronics Center, School of Engineering, The University of Tokyo, 7-3-1 Hongo, Bunkyo-ku, Tokyo 113-8656, Japan*

(Received 10 August 2017; published 20 February 2018)

We propose general methodology of deterministic single-mode quantum interaction nonlinearly modifying single quadrature variable of a continuous-variable system. The methodology is based on linear coupling of the system to ancillary systems subsequently measured by quadrature detectors. The nonlinear interaction is obtained by using the data from the quadrature detection for dynamical manipulation of the coupling parameters. This measurement-induced methodology enables direct realization of arbitrary nonlinear quadrature interactions without the need to construct them from the lowest-order gates. Such nonlinear interactions are crucial for more practical and efficient manipulation of continuous quadrature variables as well as qubits encoded in continuous-variable systems.

DOI: [10.1103/PhysRevA.97.022329](https://doi.org/10.1103/PhysRevA.97.022329)**I. INTRODUCTION**

Quantum technology employing quantum information processing with qubits is constrained to potentially large but always finite-dimensional Hilbert spaces [1,2]. To move beyond this limitation and fully process and simulate infinite-dimensional systems one has to take advantage of continuous-variable (CV) methods [3,4]. Moreover, CV methods are suitable for manipulating qubits encoded in the subspace of infinite-dimensional systems [5–7]. Such a hybrid qubit-CV approach has turned out to have practical advantages in quantum optics since it can take advantage of robust encoding of qubits and deterministic operation with CV methods [7,8]. The experimentally accessible CV operations are linear transformations of continuous quadrature operators and can be constructed from Hamiltonians of up to quadratic order of the operators [9]. Such linear transformations can be deterministically performed for systems in both Gaussian and non-Gaussian states [10]. They cannot, however, provide the nonlinear non-Gaussian dynamics which is necessary for accessing the full quantum analog simulation [4] and computation [3]. For that we require elementary nonlinear transformations which require Hamiltonians with cubic or higher-order nonlinearity [11].

Gottesman, Kitaev, and Preskill (GKP) stimulated long-standing theoretical and experimental development of the missing tools required for the elementary third-order (cubic) nonlinear phase gate [6]. We have recently expanded upon the original concept by designing a deterministic cubic nonlinear phase gate for a traveling beam of light based on adaptive continuous-variable measurement and linear feedforward control [12]. Such cubic gates can be used as elements in a suitable

sequence of noncommuting unitary operators that, together with available linear gates, can be used for realization of an arbitrary unitary operator of CV systems [11,13]. Such operators are sufficient for universal computing with both CV and, through the hybrid approach [7], qubit quantum systems. However, even though the cubic gates can be used in this capacity, it is not always practical as the number of required elementary gates quickly grows with the order of the desired nonlinearity. For example, the fourth-order Kerr nonlinearity necessary for realizing controlled-NOT gates of qubits, quantum nondemolition measurement of photon number [14], and creation of Schrödinger cat states [15] requires tens of individual cubic or lower-order gates in order to be realized with sufficient precision [16]. Operations of even higher orders are required for universal processing of CV quantum systems. Hybrid implementation of unitary quantum Toffoli gate for qubits [2,17] demands nonlinearity of the sixth-order and unitary gates for manipulation with CV encoded qubits have even stronger requirements [18]. Beyond quantum computing, such high-order operations would also allow quantum simulation of exotic dynamics [5] and open up new possibilities for manipulating quantum information. However, composing these higher-order gates from the lowest-order elements quickly becomes experimentally intractable as the order increases. Fortunately, the number of required operations can be dramatically decreased if at least some of the high-order nonlinear operations can be implemented directly [16].

In this paper we present a full methodology for directly realizing deterministic nonlinear quadrature phase gates of an arbitrary order. These gates require a set of ancillary harmonic oscillators linearly coupled to the target system and measured by quadrature detectors. The required nonlinearity is obtained by nonlinear classical feedforward control [19]. In order to compensate for quantum noise appearing due to the deterministic nature of the gates, the ancillary oscillators

\*marek@optics.upol.cz

†akiraf@ap.t.u-tokyo.ac.jp

need to be initialized in *nonlinearly squeezed states*. Such states can be prepared in advance by probabilistic methods [20] or on different platforms and stored before they are needed [21,22]. We will describe the overall strategy and then focus on the illustrative example of the fourth-order (quartic) nonlinear gate. The proposal is implementable with the current optical hybrid technology [7] and can be incorporated into a scalable architecture for optical quantum computing [23], making it suitable for efficient realization of universal quantum computing with qubits and CVs. It can be also adapted to other physical platforms, such as phononic modes in quantum electromechanical and optomechanical systems [24], motion modes of trapped ions [25], microwave radiation in cavity QED [26], or collective spins of atoms [27,28].

## II. CV QUANTUM OPERATIONS

The ultimate tool of CV quantum information processing is a unitary transformation realizing dynamics of an arbitrary Hamiltonian [11]. For CV harmonic oscillators, which are described with the help of quadrature operators  $\hat{x}$  and  $\hat{p}$ , with  $[\hat{x}, \hat{p}] = i$ , the arbitrary Hamiltonian can be expressed as a bivariate polynomial  $\hat{H} = \sum_{k,l} c_{k,l}(\hat{x}^k \hat{p}^l + \hat{p}^l \hat{x}^k)$ . The elementary technique that allows construction of such operators relies on using a number of simple operations and merging them together as

$$e^{iA} e^{iB} e^{-iA} e^{-iB} \approx e^{\frac{i}{2}[A,B]}. \quad (1)$$

This technique, originally presented in [11] and in larger detail studied in [13,16], allows combining operations with different Hamiltonians into their composites. When the orders of the constituent Hamiltonians are  $N_A$  and  $N_B$ , the resulting Hamiltonian is of the order  $N = N_A + N_B - 2$ . This means that combining operations of at least third order is capable of creating an operation with order higher than that of its constituents, which can ultimately lead to creation of operations with arbitrary orders. The most elementary operation suitable for this operation is the cubic phase gate with Hamiltonian  $\hat{H} \propto \hat{x}^3$  [11,12]. However, as the order of the desired operation grows, we can start encountering scaling issues. The exact quantity of required operations strongly depends on their specific forms, but, for example, realizing operation of 10th order requires *at least*  $2^6$  individual third-order operations [29]. This issue could be resolved by realizing at least some of the higher-order operations directly, without the need to construct them from the lowest-level components repeatedly using formula (1).

In the Heisenberg representation, the cubic phase gate transforms operators of a quantum state as  $\hat{x}' = \hat{x}$  and  $\hat{p}' = \hat{p} - 3\chi_3 \hat{x}^2$ , where  $\chi_3$  is the cubic interaction gain. It can be realized by a quantum circuit depicted in Fig. 1(a). The two oscillators, the signal and the ancilla, are coupled through a QND gate, which is characterized by interaction Hamiltonian  $H_{\text{QND}} = \hat{x} \hat{p}_a$ . The  $\hat{x}_a$  quadrature of the ancilla is then measured and the obtained value is used to drive feedforward corrections of the first (displacement) and second (squeezing) orders. The coupling and the feedforward operations are individually Gaussian, but the ancillary state  $A_3$  is not. In order to compensate for the backaction noise, the ancilla  $A_3$  has to be prepared in the *cubic squeezed state*, which has fluctuations of operator

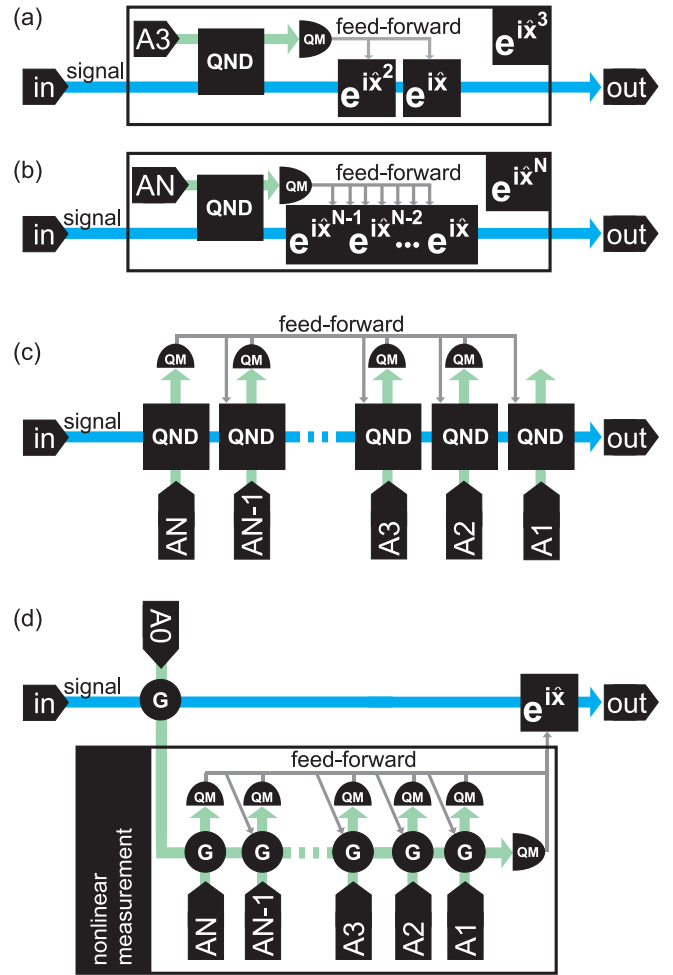


FIG. 1. Schematic circuits for various implementations of nonlinear gates. QND: quantum nondemolition interaction; QM: quadrature measurement;  $A_k$ : ancillary state of the  $k$ th order squeezed in  $\hat{p} - N\chi_N \hat{x}^{N-1}$ .  $e^{ix^k}$ : unitary realization of  $k$ th-order nonlinear gate with arbitrary strength. (a) Cubic phase gate with  $N = 3$ ; (b)  $(N + 1)$ th-order gate implemented recursively; (c)  $N$ th-order gate with streamlined feedforward; (d)  $N$ th-order gate implemented in the measurement induced way.  $G$  represents a tunable Gaussian operation, which can be either QND or beam splitter.  $A_0$  is ancillary state squeezed in  $\hat{x}$ .

$\hat{p}_a - 3\chi_3 \hat{x}_a^2$ , where the parameter  $\chi_3$  sets the strength of the nonlinearity, reduced and ideally approaching zero.

The principle can be extended to nonlinear Hamiltonians of higher order,  $\hat{H} \propto \hat{x}^N$ . They can be realized by employing an ancilla with reduced fluctuations in quadrature  $\hat{p} - N\chi_N \hat{x}^{N-1}$ . However, in this case, the required feedforward operations are of orders  $1, \dots, N - 1$ , see Fig. 1(b), and each of them requires an ancilla squeezed in a specific nonlinear quadrature. So, while the same method can be used for realizing these lower-order nonlinear circuits in such a recursive manner, the total number of gates required for realizing operation of  $N$ th order is  $2^{N-3}$ , which is again the undesirable exponential scaling.

Fortunately it is possible to merge the required feedforward operations so that only  $N - 2$  individual nonlinear gates are needed in total. The scheme is depicted in Fig. 1(c) and it

relies on a sequence of  $N$  QND interactions with  $N$  ancillary states with reduced fluctuations in quadratures  $\hat{p}_{Ak} - \xi_k \hat{x}_{Ak}^{-1}$ , where  $k = 1, \dots, N$  and the parameter  $\xi_k = \pm 1$  characterizes the orientation of the state. Apart from the orientation, the resource states do not depend upon the measurement results. The strengths of nonlinearities can be modified by setting the gains of the Gaussian QND operations, which can be realized by fast feedforward [19]. This is significantly more feasible than preparing tailored quantum states. Also, for  $k = 1, 2$  the required states are Gaussian and the gates are not nonlinear. As a consequence, the required operation can be usually realized in a different manner [30]. For the sake of resulting formulas, though, we are going to use the gate-based expression. The QND operations transform the quadrature operators of the signal  $s$  and the  $k$ th ancillary mode  $Ak$  according to

$$\begin{aligned} \hat{x}'_s &= \hat{x}_s, & \hat{p}'_s &= \hat{p}_s + z_k \hat{p}_{Ak}, \\ \hat{x}'_{Ak} &= \hat{x}_{Ak} - z_k \hat{x}_s, & \hat{p}'_{Ak} &= \hat{p}_{Ak}. \end{aligned} \quad (2)$$

The ancillary modes are then measured, yielding values  $q_k = \hat{x}_{Ak} - z_k \hat{x}_s$ . The gains  $z_k$  of the QND operations are going to be functions of the previously measured values. To find them, we can express the final quadrature relations as

$$\hat{x}_{\text{out}} = \hat{x}_{\text{in}}, \quad \hat{p}_{\text{out}} = \hat{p}_{\text{in}} + \sum_{j=1}^N z_j \hat{p}_{Aj}, \quad (3)$$

where  $z_j$  are yet to be determined. We can use the nonlinear property of ancillary states and the relationship between the operators and the measured quadratures,

$$\hat{p}_{Ak} = \xi_k \hat{x}_{Ak}^{k-1}, \quad \hat{x}_{Ak} = z_k \hat{x}_{\text{in}} + q_k, \quad (4)$$

where  $q_k$  are the values obtained by the quadrature detectors, and arrive at the final form of the  $\hat{p}$ -quadrature relations as

$$\begin{aligned} \hat{p}_{\text{out}} &= \hat{p}_{\text{in}} + \sum_{k=0}^{N-1} \hat{x}_{\text{in}}^k \sum_{j=1}^{N-k} \xi_{N-j+1} \binom{N-j}{k} \\ &\times (q_{N-j+1})^{N-j-k} (z_{N-j+1})^{k+1}. \end{aligned} \quad (5)$$

We can see that transformation given by (3) and (5) realizes the desired  $\hat{x}^N$  operation when the QND gain is proportional to the desired nonlinear operation gain,  $(z_N)^N = N \chi_N$  with  $\xi_N = 1$ , and the remaining gains satisfy a set of  $N - 1$  equations

$$\sum_{j=1}^{N-k} \xi_{N-j+1} \binom{N-j}{k} (q_{N-j+1})^{N-j-k} (z_{N-j+1})^{k+1} = 0 \quad (6)$$

for all  $k = 0, \dots, N - 2$ . This is a set of polynomial equations for  $z_j$ , which is already in the upper diagonal form and has always a unique solution when the parameters  $\xi_j$  can be adjusted. More importantly, the solution can be found in a recurrent form, so values of each  $z_j$  and  $\xi_j$  are functions only of the already known quantities  $z_m, \xi_m$ , and  $q_m$ , where  $m > j$ . Also note that the measured value  $q_1$  is not needed and the measurement therefore does not need to be performed.

For feasible tests of the operation which could be performed in the near future we can consider engineering the resource states approximatively by assembling them in a limited Hilbert space [12,31]. This can be done with optical detectors [20,32,33] or, for larger number of ancillas, with the help of two-level quantum systems [34,35]. The available

dimension of the Hilbert space sets limits to the fluctuations of the nonlinear quadrature and higher orders of nonlinearity require more ancillary photons or two-level systems to reach the same squeezing of residual noise. However, when the available dimensions of the Hilbert spaces for each of the resource states are equal, the noise added during the direct implementation of a single high-order operation tends to be lower than if the operation was constructed from the lower-order gates (see the Appendixes for the details).

### III. NONLINEAR MEASUREMENT-INDUCED APPROACH

Applying elementary quantum circuits directly to a quantum state is a very straightforward approach. However, in practice it is often beneficial to take advantage of the inherent entangling property of quantum states and impress the desired nonlinearity onto the states through a suitable measurement performed on a suitable subsystem. So while the components of the circuit in Fig. 1(c) already follow the measurement-induced paradigm, it is sensible to take this path to its logical conclusion and perform the full gate completely through a measurement. The scheme is sketched in Fig. 1(d) and it consists of a single QND interaction coupling together the initial system with ancillary system  $A_s$  prepared in a sufficiently squeezed vacuum state. This ancillary system is then subjected to the in-line nonlinear gate consisting of QND gates with parameters  $z_k$  coupling the system to  $N$  ancillary states, which are subsequently measured by  $\hat{x}$ -quadrature detectors. In addition, the remaining ancillary mode is measured by a  $\hat{p}$ -quadrature measurement, which is used to erase the influence of the carrier ancilla. The individual  $\hat{x}$ -quadrature measurements provide measurement results  $q_k = \hat{x}_k - z_k \hat{x}_{\text{in}}$ . After the initial system is displaced by the measured value of the final  $\hat{p}$ -quadrature measurement,  $y = \hat{p}_0 + \sum_{k=1}^N \hat{p}_{Ak}$ , the quadrature operators of the initial system can be exactly described by (3) and therefore subsequently corrected in the same manner. Under ideal conditions the measurement-induced and the in-line schemes are mathematically equivalent.

The QND coupling can be also replaced by a symmetric passive linear coupling, which is described by interaction Hamiltonian  $\hat{H}_{BS} \propto \hat{x}_1 \hat{p}_2 + \hat{p}_1 \hat{x}_2$ . This coupling, which for optical systems stands for the ubiquitous beam splitter, is passive; it only transfers energy between the systems instead of creating it. As a consequence, it is often more feasible and less prone to noise and imperfections, and at optical frequencies it can work with arbitrarily high speed. On the other hand, the mixing of both quadratures makes it often more difficult to treat, as compared to the QND. In our scenario, however, the operations can be made equivalent. To see this, let us again consider the measurement-induced scheme of Fig. 1(d). The first beam splitter can have an arbitrary transmissivity  $t_0$ . However, it is also preceded by the Gaussian squeezing operation, which ensures that  $\hat{x}_{\text{out}} = \hat{x}_{\text{in}}$ . After the ancillary state  $A_0$  interacts with the first beam splitter of the nonlinear measurement block, with positive transmissivity  $t_N$  and reflectivity  $r_N$ , its quadratures transform to

$$\hat{x}_{A_0}^{(N)} = t_N \hat{x}_{\text{in}} + r_N \hat{x}_{AN}, \quad \hat{p}_{A_0}^{(N)} = t_N \hat{p}_{\text{in}} + r_N \hat{p}_{AN}, \quad (7)$$

and the  $\hat{x}$  quadrature measurement of the nonlinear ancilla provides value  $q_N = t_N \hat{x}_{AN} - r_N \hat{x}_{\text{in}}$ . In order to simplify the

description we can now use this measured value and use it to transform the state (7) by Gaussian displacement and squeezing into

$$\hat{x}_{A0}^{(N)'} = \hat{x}_{\text{in}}, \quad \hat{p}_{A0}^{(N)'} = t_N^2 \hat{p}_{\text{in}} + t_N r_N \hat{p}_{A_N}. \quad (8)$$

Since these operations are Gaussian, as is the rest of the active components of the circuit, it is enough to consider them virtually and include their influence only into the measured data. Here we treat them as physical operations to simplify the derivation. After the sequence of all  $N$  beam splitters and erasing the influence of the carrier ancilla, the quadrature operators of the signal can be expressed as

$$\hat{x}_{\text{out}} = \hat{x}_{\text{in}}, \quad \hat{p}_{\text{out}} = \hat{p}_{\text{in}} + \sum_{j=1}^N \left( t_j r_j \prod_{k=j}^N t_k^{-2} \right) \hat{p}_{A_j}. \quad (9)$$

The form is again equivalent to (3). The coefficients  $t_j r_j \prod_{k=j}^N t_k^{-2}$  which need to be compensated are more involved than in the previous scenarios, but the final set of equations for the beam splitter coefficients can be solved in the same manner as for the QND scenario.

#### IV. QUARTIC NONLINEARITY

This specific gate, a step above the elementary cubic nonlinearity, is strongly beneficial in realization of Kerr nonlinearity [16]. The particular linear optical scheme is in Fig. 2. The implementation follows the steps drawn in the general section with only few differences. The ancillary states are prepared with squeezing in quadratures  $\hat{p}_{A_k} - k\chi_k \hat{x}_{A_k}^{k-1}$ , where the parameters  $\chi_k$  are not related to the strength of the nonlinearity and only represent additional degrees of freedom which can be exploited during the preparation. The squeezing operations (8) previously considered to simplify the description are missing. The last two blocks corresponding to ancillas of orders 1 and 2 are also missing; these two operations are Gaussian and are

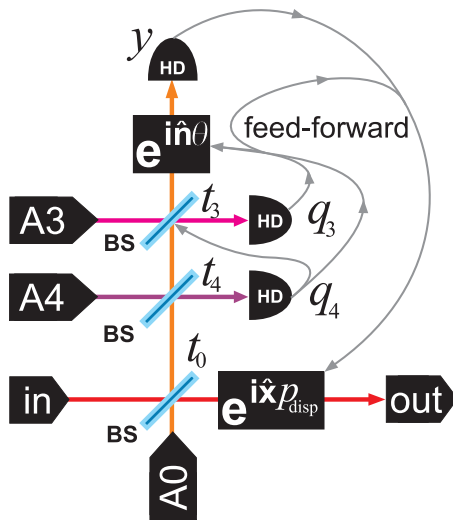


FIG. 2. Scheme for the optical realization of the fourth-order nonlinear circuit. BS: beam splitter; HD: homodyne detection;  $e^{i\hat{n}\theta}$ : operation realizing  $\theta$  phase shift;  $e^{i\hat{x}p_{\text{disp}}}$ :  $\hat{p}$ -quadrature displacement by value  $p_{\text{disp}}$ ;  $t_0, t_4, t_3$ : splitting ratios of respective beam splitters;  $y, q_4, q_3$ : values measured by the homodyne detectors.

therefore implemented in another way. The displacement is implemented directly. The squeezing is realized by adaptive measurement of the quadrature rotated by  $\theta$ , which is a parameter that depends on previous measurement results [30]. The three values measured by the optical homodyne detectors are

$$q_4 = -r_0 r_4 \hat{x}_{\text{in}} - t_0 r_4 \hat{x}_{A0} + t_4 \hat{x}_{A4}, \quad (10)$$

$$q_3 = -r_0 t_4 r_3 \hat{x}_{\text{in}} - t_0 t_4 r_3 \hat{x}_{A0} - r_4 r_3 \hat{x}_{A4} + t_3 \hat{x}_{A3}, \quad (11)$$

$$y = \sin \theta (r_0 t_4 t_3 \hat{x}_{\text{in}} + t_0 t_4 t_3 \hat{x}_{A0} + r_4 t_3 \hat{x}_{A4} + r_3 \hat{x}_{A3}) \\ + \cos \theta (r_0 t_4 t_3 \hat{p}_{\text{in}} + t_0 t_4 t_3 \hat{p}_{A0} + r_4 t_3 \hat{p}_{A4} + r_3 \hat{p}_{A3}). \quad (12)$$

The splitting ratio of the second beam splitter, as well as the required phase shift, depend on the already measured results:

$$\chi_3 \left( \frac{r_3}{t_3} \right)^3 = -\frac{4\chi_4 r_4^3}{t_4} q_4, \quad (13)$$

$$\tan \theta = -\frac{6\chi_3 r_3^2}{t_3} q_3 - \frac{12\chi_4 r_4^2 t_3^2}{t_4^2} (t_4^2 - r_4^2) q_4^2, \quad (14)$$

and fast electronic circuits [7] are required to process the data quickly enough to provide the required feedforward. Finally, the remaining signal state needs to be displaced by a single value,

$$p_{\text{disp}} = -\frac{4\chi_4 r_0 r_4}{t_0 t_4^4} q_4^3 - \frac{3\chi_3 r_0 r_3}{t_0 t_4 t_3^3} \left( \frac{r_4 r_3}{t_4} q_4 + q_3 \right)^2 \\ - \frac{r_0 r_4}{t_0 t_4^2 t_3^2} \tan \theta \left( q_4 + \frac{t_4 r_3}{r_4} q_3 \right) + \frac{r_0}{t_0 t_4 t_3 \cos \theta} q_2, \quad (15)$$

in order to transform the output quadrature operators to

$$\hat{x}_{\text{out}} = t_0 \hat{x}_{\text{in}} - r_0 \hat{x}_{A0}, \quad (16a)$$

$$\hat{p}_{\text{out}} = \frac{1}{t_0} \left[ \hat{p}_{\text{in}} + \frac{4\chi_4 r_0^4 r_4^4}{t_4^4} \left( \hat{x}_{\text{in}} + \frac{t_0}{r_0} \hat{x}_{A0} \right)^3 \right] \\ + \frac{r_0 r_4}{t_0 t_4} (\hat{p}_{A4} - 4\chi_4 \hat{x}_{A4}^3) \\ + \frac{r_0 r_4}{t_0 t_4} \left[ \frac{4\chi_4}{\chi_3 t_4} (r_0 r_4 \hat{x}_{\text{in}} + t_0 r_4 \hat{x}_{A0} - t_4 \hat{x}_{A4}) \right]^{\frac{1}{3}} \\ \times (\hat{p}_{A3} - 3\chi_3 \hat{x}_{A3}^2). \quad (16b)$$

We can see that the operators correspond to the input signal, squeezed by factor  $t_0$ , transformed by the fourth-order nonlinear phase gate with effective strength  $\chi_4' = \frac{4\chi_4 r_0^4 r_4^4}{t_4^4}$ . The remaining terms represent the imperfections arising from ancillary states—both the finite linear squeezing in the mode  $A0$  and the finite nonlinear squeezing in modes  $A4$  and  $A3$ . The last term depends on the input state as well as both nonlinear ancillas, which are caused by the coupling parameter  $t_3$  depending on the measurement of  $A4$ . As a consequence, if we assume that the input state is suitably limited in the phase space, for good performance the nonlinear ancillary states should satisfy

$$\left[ \Delta(\hat{p}_{A3} - 3\chi_3 \hat{x}_{A3}^2) \right]^2 \ll \frac{1}{\left[ \Delta \hat{x}_{A4}^{\frac{1}{3}} \right]^2}. \quad (17)$$

This represents an example of the squeezing requirement for a new class of nonlinear squeezed states. The dynamical problem of implementing any nonlinear phase gate has been therefore turned into the static problem of preparing suitable quantum resource states.

## V. CONCLUSION

The presented methodology has two revolutionary advantages over the previous methods. First, further integration of feedforward to adjust the coupling coefficients allows one to manipulate with strengths of the nonlinear operation by using only Gaussian tools. As a consequence, there is no need to prepare nonlinear quantum states for specific strengths of the nonlinearity, which significantly streamlines the state preparation phase of the circuit, as it moves all non-Gaussian requirements to preparation of *only* universal single-mode nonlinear squeezed states. Second, the ability to merge the necessary feedforwards into a single sequence removes the exponential scaling in the number of operations. The higher-order ancillary states exhibit more complex quantum superpositions, but reducing their overall number leads both to easier implementation and better performance. Together these innovations with the current development of time-resolved optical quantum technology [22] open up the possibility of feasible and efficient experimental realization of the nonlinear phase gates and their application to CV simulation and hybrid qubit-CV computation [3–5,7].

## ACKNOWLEDGMENTS

This work was partly supported by Core Research for Evolutional Science and Technology (CREST) (Grant No. JP-MJCR15N5) of Japan Science and Technology Agency (JST), Japan Society for the Promotion of Science (JSPS) KAKENHI, APSA. H.O. acknowledges financial support from ALPS. P.M. acknowledges project LTC17086 of INTER-EXCELLENCE program of Czech Ministry of Education. R.F. acknowledges Project No. GB14-36681G of the Czech Science Foundation.

## APPENDIX A: APPROXIMATIVE NONLINEAR SQUEEZED STATES

The deterministic nonlinear quadrature phase gates require resource states that are squeezed in a specific nonlinear quadrature. Gate implementing operation  $\hat{x}^N$  needs states for which the quadrature moment given by  $\langle [\Delta(\hat{p} - \hat{x}^{N-1})]^2 \rangle$  is reduced and ideally approaching zero. Such states can be approximatively prepared by constructing specific states in a limited dimensional Hilbert space and then suitably shaping them by Gaussian operations [31]. The optimal form can be found by extending the approach of [30] and finding the minimum eigenvalue and the corresponding eigenstate of operator

$$\hat{Y}(\lambda, d) = \sum_{m=0, n=0}^{D-1} \langle m | [\hat{y}(\lambda) - d]^2 | n \rangle | m \rangle \langle n |, \quad (\text{A1})$$

where  $N$  is the order of the required nonlinearity,  $D$  is the available dimension of the Hilbert space, and

$$\hat{y}(\lambda) = \lambda \hat{p} - \left( \frac{\hat{x}}{\lambda} \right)^{N-1}. \quad (\text{A2})$$

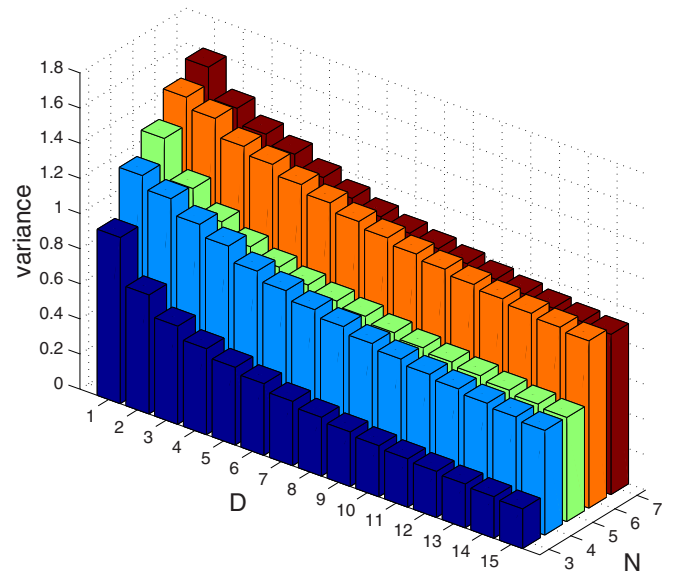


FIG. 3. Variances of the nonlinear quadrature  $\hat{y}_{AN} = \hat{p} - \hat{x}^{N-1}$  for states prepared in a limited Hilbert space with dimension  $D$ .

The real parameters  $\lambda$  and  $d$  are optimized over and correspond to the corrective Gaussian operations of squeezing ( $\lambda$ ) and displacement ( $d$ ) applied to the produced state. We have performed the optimization and the minimal variances obtainable for varying dimension of the Hilbert space are shown in Fig. 3.

## APPENDIX B: COMPARISON OF DIFFERENT ARCHITECTURES FOR IMPLEMENTATION OF THE QUARTIC GATE

Beside the direct approach we are advocating in the manuscript, high-order nonlinear gates can be also composed as a sequence of nonlinear gates of lower order [13]. The number of required lower-order gates is substantially higher, but they are easier to implement. The comparison of the two methods can be made in terms of the total amount of excess noise that gets added during the implementation. The excess noise depends on the architecture of the gate and on the properties of the nonlinear ancillary states, which are ideally squeezed in the nonlinear quadratures  $\hat{y}_{AN} = \hat{p} - \hat{x}^{N-1}$ .

Let us consider an example of the quartic operation with Hamiltonian  $\hat{H} = \chi_4 \hat{x}^4$ . According to [13] it can be decomposed into a sequence of six cubic gates and four Gaussian gates as per

$$[-\epsilon \hat{x}^3, [\epsilon \hat{x}^3, \epsilon \hat{p}^2]] = \frac{9}{2} \epsilon^3 \hat{x}^4, \quad (\text{B1})$$

where  $\epsilon = (\frac{2\chi_4}{9})^{1/3}$ . In principle, each of the three operations used in the sequence could have a different coupling constant, but they would all have to be much smaller than one and the total interaction strength  $\chi_4$  would be always proportional to their product. In practical scenarios, detailed optimization over the three parameters would probably improve performance, but for the purpose of this benchmark we will consider them equal, because this scenario maximizes their product. If we neglect the error terms proportional to  $\epsilon^4$  and assume that the Gaussian gates can be realized perfectly, only the cubic gates contribute

to the noise, each one by

$$\mathcal{N}_3 = (2\epsilon)^{2/3} \langle (\Delta \hat{y}_{A3})^2 \rangle. \quad (\text{B2})$$

In total, the noise contributes to different quadratures, but the total amount is  $\mathcal{N}_{\text{dec}} = 6\mathcal{N}_3$ . It should be also noted that separating the operation into two sequences, each one with half the strength of the total, generally leads to a higher amount of added noise and is therefore unpractical.

If we are attempting to realize the same operation directly, according to our proposal, the output quadrature can be found as (5):

$$\hat{p}_{\text{out}} = \hat{p}_{\text{in}} + 4\chi_4 \hat{x}_{\text{in}}^3 - z_4 \hat{y}_{A4} - z_3 \hat{y}_{A,3}, \quad (\text{B3})$$

where  $z_4 = (4\chi_4)^{1/4}$  and  $z_3 = -[9\chi_4(\hat{x}_{A4} - z_4 \hat{x}_0)]^{1/3}$  and we have neglected the terms which can be corrected by Gaussian operations. The total added noise can be then estimated to be

$$\mathcal{N}_{\text{dir}} = (4\chi_4)^{1/2} \langle (\Delta \hat{y}_{A4})^2 \rangle + (9\chi_4)^{2/3} \langle (\hat{x}_{A4} - z_4 \hat{x}_{\text{in}})^2 \rangle \langle (\Delta \hat{y}_{A3})^2 \rangle. \quad (\text{B4})$$

To compare these two expressions we need to set some assumptions about our system. We shall consider  $\chi_4 = 0.1$  and an input state which has distribution of the  $\hat{x}_{\text{in}}$  quadrature given

by Gaussian function with zero mean and variance  $\Delta^2 = 5$ . The second assumption is relevant for (B3), because the input state affects the distribution of  $z_3$ . Keep in mind that any state which in the  $x$  representation is narrower than the assumed function would receive less noise. Finally, for our resource states, we shall consider realistic approximations with  $D = 4$ , which can be feasibly prepared already with the present technology. In this dimension, the minimal variances are, as can be seen in Fig. 3,  $\langle (\Delta \hat{y}_{A3})^2 \rangle \approx 0.5$  and  $\langle (\Delta \hat{y}_{A4})^2 \rangle \approx 1$ .

Under these assumptions, the amounts of total added noise can be estimated to be

$$\mathcal{N}_{\text{dec}} \approx 4.1 \langle (\Delta \hat{y}_{A3})^2 \rangle \approx 2 \quad (\text{B5})$$

and

$$\mathcal{N}_{\text{dir}} \approx 0.63 \langle (\Delta \hat{y}_{A4})^2 \rangle + 1.12 \langle (\Delta \hat{y}_{A3})^2 \rangle \approx 1.2. \quad (\text{B6})$$

We can therefore see that the proposed direct scheme suggests superior performance even though the total Hilbert space of the resource states is significantly smaller,  $D^2 < D^6$ . This statement remains true for all the checked dimensions, up to  $D = 15$ . This result is immediately relevant for the first proof-of-principle experiments aimed at demonstrating exotic higher-order quantum nonlinearities.

- 
- [1] D. Gottesman, Theory of fault-tolerant quantum computation, *Phys. Rev. A* **57**, 127 (1998).
  - [2] M. A. Nielsen and I. L. Chuang, *Quantum Computation and Quantum Information* (Cambridge University Press, Cambridge, UK, 2005).
  - [3] S. L. Braunstein and P. van Loock, Quantum information with continuous variables, *Rev. Mod. Phys.* **77**, 513 (2005); C. Weedbrook, S. Pirandola, R. Garcia-Patron, N. J. Cerf, T. C. Ralph, J. H. Shapiro, and S. Lloyd, Gaussian quantum information, *ibid.* **84**, 621 (2012).
  - [4] V. M. Kendon, K. Nemoto, and W. J. Munro, Quantum analogue computing, *Philos. Trans. R. Soc. A* **368**, 3609 (2010); I. M. Georgescu, S. Ashhab, and F. Nori, Quantum simulation, *Rev. Mod. Phys.* **86**, 153 (2014).
  - [5] K. Marshall, R. Pooser, G. Siopsis, and C. Weedbrook, Quantum simulation of quantum field theory using continuous variables, *Phys. Rev. A* **92**, 063825 (2015).
  - [6] D. Gottesman, A. Kitaev, and J. Preskill, Encoding a qubit in an oscillator, *Phys. Rev. A* **64**, 012310 (2001).
  - [7] A. Furusawa and P. van Loock, *Quantum Teleportation and Entanglement: A Hybrid Approach to Optical Quantum Information Processing* (Wiley, New York, 2011).
  - [8] S. Takeda, T. Mizuta, M. Fuwa, P. van Loock, and A. Furusawa, Deterministic quantum teleportation of photonic quantum bits by a hybrid technique, *Nature (London)* **500**, 315 (2013).
  - [9] R. Filip, P. Marek, and U. L. Andersen, Measurement-induced continuous-variable quantum interactions, *Phys. Rev. A* **71**, 042308 (2005); S. L. Braunstein, Squeezing as an irreducible resource, *ibid.* **71**, 055801 (2005).
  - [10] Y. Miwa, J. Yoshikawa, N. Iwata, M. Endo, P. Marek, R. Filip, P. van Loock, and A. Furusawa, Exploring a New Regime for Processing Optical Qubits: Squeezing and Unsqueezing Single Photons, *Phys. Rev. Lett.* **113**, 013601 (2014).
  - [11] S. Lloyd and S. L. Braunstein, Quantum Computation over Continuous Variables, *Phys. Rev. Lett.* **82**, 1784 (1999).
  - [12] P. Marek, R. Filip, and A. Furusawa, Deterministic implementation of weak quantum cubic nonlinearity, *Phys. Rev. A* **84**, 053802 (2011).
  - [13] S. Sefi and P. van Loock, How to Decompose Arbitrary Continuous-Variable Quantum Operations, *Phys. Rev. Lett.* **107**, 170501 (2011).
  - [14] N. Imoto, H. A. Haus, and Y. Yamamoto, Quantum nondemolition measurement of the photon number via the optical Kerr effect, *Phys. Rev. A* **32**, 2287 (1985).
  - [15] B. Yurke and D. Stoler, Generating Quantum Mechanical Superpositions of Macroscopically Distinguishable States via Amplitude Dispersion, *Phys. Rev. Lett.* **57**, 13 (1986).
  - [16] S. Sefi, V. Vaibhav, and P. van Loock, Measurement-induced optical Kerr interaction, *Phys. Rev. A* **88**, 012303 (2013).
  - [17] M. Mičuda, M. Sedlák, I. Straka, M. Miková, M. Dušek, M. Ježek, and J. Fiurášek, Efficient Experimental Estimation of Fidelity of Linear Optical Quantum Toffoli Gate, *Phys. Rev. Lett.* **111**, 160407 (2013).
  - [18] T. C. Ralph, A. Gilchrist, G. J. Milburn, W. J. Munro, and S. Glancy, Quantum computation with optical coherent states, *Phys. Rev. A* **68**, 042319 (2003).
  - [19] K. Miyata, H. Ogawa, P. Marek, R. Filip, H. Yonezawa, J. Yoshikawa, and A. Furusawa, Experimental realization of a dynamic squeezing gate, *Phys. Rev. A* **90**, 060302(R) (2014).
  - [20] M. Yukawa, K. Miyata, H. Yonezawa, P. Marek, R. Filip, and A. Furusawa, Emulating quantum cubic nonlinearity, *Phys. Rev. A* **88**, 053816 (2013).
  - [21] A. I. Lvovsky, B. C. Sanders, and W. Tittel, Optical quantum memory, *Nat. Photon.* **3**, 706 (2009).
  - [22] K. Makino, Y. Hashimoto, J. Yoshikawa, H. Ohdan, T. Toyama, P. van Loock, and A. Furusawa, Synchronization of optical

- photons for quantum information processing, *Sci. Adv.* **2**, e1501772 (2016).
- [23] S. Takeda and A. Furusawa, Universal Quantum Computing with Measurement-Induced Continuous-Variable Gate Sequence in a Loop-Based Architecture, *Phys. Rev. Lett.* **119**, 120504 (2017).
- [24] E. Verhagen, S. Deléglise, S. Weis, A. Schliesser, and T. J. Kippenberg, Quantum-coherent coupling of a mechanical oscillator to an optical cavity mode, *Nature (London)* **482**, 63 (2012); T. A. Palomaki, J. D. Teufel, R. W. Simmonds, and K. W. Lehnert, Entangling mechanical motion with microwave fields, *Science* **342**, 710 (2013).
- [25] D. Leibfried, R. Blatt, C. Monroe, and D. Wineland, Quantum dynamics of single trapped ions, *Rev. Mod. Phys.* **75**, 281 (2003).
- [26] A. Reiserer and G. Rempe, Cavity-based quantum networks with single atoms and optical photons, *Rev. Mod. Phys.* **87**, 1379 (2015).
- [27] I. D. Leroux, M. H. Schleier-Smith, and V. Vuletić, Implementation of Cavity Squeezing of a Collective Atomic Spin, *Phys. Rev. Lett.* **104**, 073602 (2010).
- [28] T. Opatrný, Quasi-continuous variable quantum computation with collective spins in multi-path interferometers, *Phys. Rev. Lett.* **119**, 010502 (2017).
- [29] Operation of 10th order requires  $2^2$  sixth-order operations, which is  $2^4$  fourth-order operations or  $2^6$  third-order operations.
- [30] K. Miyata, H. Ogawa, P. Marek, R. Filip, H. Yonezawa, J. Yoshikawa, and A. Furusawa, Implementation of a quantum cubic gate by an adaptive non-Gaussian measurement, *Phys. Rev. A* **93**, 022301 (2016).
- [31] D. Menzies and R. Filip, Gaussian-optimized preparation of non-Gaussian pure states, *Phys. Rev. A* **79**, 012313 (2009).
- [32] M. Cooper, L. J. Wright, C. Söller, and B. J. Smith, Experimental generation of multi-photon Fock states, *Opt. Exp.* **21**, 5309 (2013).
- [33] M. Yukawa, K. Miyata, T. Mizuta, H. Yonezawa, P. Marek, R. Filip, and A. Furusawa, Generating superposition of up-to three photons for continuous variable quantum information processing, *Opt. Exp.* **21**, 5529 (2013).
- [34] S. Deléglise, I. Dotsenko, C. Sayrin, J. Bernu, M. Brune, J. M. Raimond, and S. Haroche, Reconstruction of non-classical cavity field states with snapshots of their decoherence, *Nature (London)* **455**, 510 (2008).
- [35] B. Vlastakis, G. Kirchmair, Z. Leghtas, S. E. Nigg, L. Frunzio, S. M. Girvin, M. Mirrahimi, M. H. Devoret, and R. J. Schoelkopf, Deterministically encoding quantum information using 100-photon Schrödinger cat states, *Science* **342**, 607 (2013).